

Non-Markovian Effects in Quantum Rate Calculations of Hydrogen Diffusion with Electronic Friction

George Trenins* and Mariana Rossi
MPI for the Structure and Dynamics of Matter,
Luruper Chaussee 149, 22761 Hamburg, Germany
(Dated: December 20, 2024)

We address the challenge of incorporating non-Markovian electronic friction effects in quantum-mechanical approximations of dynamical observables. A generalized Langevin equation (GLE) is formulated for ring-polymer molecular dynamics (RPMD) rate calculations, which combines electronic friction with a description of nuclear quantum effects (NQEs) for adsorbates on metal surfaces. An efficient propagation algorithm is introduced that captures both the spatial dependence of friction strength and non-Markovian frictional memory. This framework is applied to a model of hydrogen diffusing on Cu(111) derived from *ab initio* density functional theory (DFT) calculations, revealing significant alterations in rate constants and tunnelling crossover temperatures due to non-Markovian effects. Our findings explain why previous classical molecular dynamics simulations with Markovian friction showed unexpectedly good agreement with experiment, highlighting the critical role of non-Markovian effects in first-principles atomistic simulations.

Introduction.—Dissipative forces, *i.e.*, friction, arising from dynamical coarse-graining, play a crucial role in modelling multi-timescale systems [1]. A wide range of phenomena, including charge-transfer reactions in polar solvents, vibrational relaxation in liquids, and interfacial dynamics, can be effectively described as dissipative rate processes [2–4]. In particular, the dynamics of molecules on metal surfaces, influenced by electron–nuclear nonadiabatic coupling, are well-captured by electronic friction models [5–7]. While classical molecular dynamics with electronic friction (MDEF) has been successfully applied to various problems, such as vibrational relaxation [8], dissociative chemisorption [9], and molecule-surface scattering [10, 11], it is limited by two significant shortcomings: the neglect of NQEs and the prevalent assumption of Markovian friction.

Path integral-based methods [12] have proven especially effective at incorporating NQEs into rate calculations, with semiclassical instantons [13] and ring-polymer molecular dynamics (RPMD) [14] being standout approaches. The core strength of these methods lies in their ability to faithfully capture zero-point energy effects and incoherent quantum tunnelling, by harnessing the isomorphism between imaginary-time path integrals and the canonical partition function of an extended classical system [15]. This makes them very efficient and enables the inclusion of NQEs into simulations of multi-dimensional anharmonic systems, with a computational overhead comparable to that of a geometry optimization or a classical MD simulation in an extended phase space.

A semiclassical instanton rate theory incorporating first-principles electronic friction was developed by Litman and co-workers [16, 17]. The theory accurately describes the tunnelling-suppressing effects of friction, but is not suited, *e.g.*, to surface dynamics in the low-friction regime, which is rate-limited by energy diffusion [18, 19]. Instanton theory struggles to accurately

capture this regime [20], adding to its inherent challenges in describing low-barrier systems and reactions above the tunnelling crossover temperature [21].

Unlike instanton theory, RPMD does not suffer from these limitations and performs well across a wide range of friction strengths, as long as coherent nuclear tunnelling remains negligible [22–24]. Benchmarks against reaction rates calculated using the multi-configuration time-dependent Hartree (MCTDH) method for model systems showed that RPMD can capture NQEs related to the spatial variation of the friction forces across a wide-range of friction strengths [24]. Recently, Bi and Dou [25] performed RPMD simulations applying frictional forces to the ring-polymer centroids and assuming Markovian friction. Under these assumptions, the dissipative dynamics could be propagated efficiently, using a modified version of the path-integral Langevin equation (PILE) propagation algorithm [26]. The restriction of frictional forces to the centroids, however, means that the suppression of the tunnelling probability is not captured [16, 17]. Furthermore, the description of non-Markovian effects is acknowledged as an outstanding challenge by the authors, highlighting the need for a more comprehensive solution.

Achieving a rigorous and, at the same time, efficient formulation of RPMD for dissipative systems thus remains an unsolved problem [24, 25]. Previously, Lawrence *et al.* [27] formulated a path-integral GLE for position-independent friction. Here, we generalize the derivation to include position-dependence of the friction and adopt the more efficient auxiliary variable propagation method [1]. This technique, explored by Ceriotti and co-workers for enhancing sampling in classical and path-integral MD [26, 28–30], is repurposed to simulate the dissipative dynamics driven by an *ab initio* electronic memory–friction kernel. Using our implementation, we analyse a model of hydrogen diffusion on Cu(111), for which earlier classical MD simulations by Gu *et al.* [31]

showed close agreement with experimental measurements at 200 K [32]. This is unexpected given the significance of zero-point energy and shallow tunnelling in such systems around room temperature [33, 34]. Our findings reveal that non-Markovian effects can explain this anomalous agreement.

Theory.—We begin by considering the classical Hamiltonian of an $(f + 1)$ -dimensional system,

$$H(\mathbf{p}, \mathbf{q}) = \sum_{\nu=0}^f \frac{p_{\nu}^2}{2m_{\nu}} + V(\mathbf{q}), \quad (1)$$

where $\mathbf{p} = (p_0, \dots, p_f)$ and $\mathbf{q} = (q_0, \dots, q_f)$ denote the Cartesian momentum and position coordinates, respectively, and V is the potential energy. To construct the RPMD Hamiltonian [35], we introduce N replicas of the original system, also referred to as beads, which are connected into a ring polymer by harmonic springs. The RPMD Hamiltonian is given by

$$H_N(\mathbf{p}, \mathbf{q}) = \sum_{l=0}^{N-1} H(\mathbf{p}^{(l)}, \mathbf{q}^{(l)}) + \sum_{\nu=0}^f S_N(\mathbf{q}_{\nu}), \quad (2)$$

where $\mathbf{q}^{(l)} = (q_0^{(l)}, \dots, q_f^{(l)})$ represents the position coordinates of the l -th replica and $\mathbf{q}_{\nu} = (q_{\nu}^{(0)}, \dots, q_{\nu}^{(l-1)})$ denotes the ν -th components of the position coordinates of all replicas. The harmonic spring term,

$$S_N(\mathbf{q}_{\nu}) = \sum_{l=0}^{N-1} \frac{m_{\nu} \omega_N^2}{2} (q_{\nu}^{(l+1)} - q_{\nu}^{(l)})^2 \quad (3)$$

depends on temperature T through the harmonic frequency $\omega_N = N/\beta\hbar$, where $\beta = 1/k_{\text{B}}T$.

In the limit of large N , typically around $\mathcal{O}(10)$ – $\mathcal{O}(100)$, the classical canonical distribution of RPMD position coordinates converges to the exact quantum Boltzmann distribution. This property, along with others discussed in Refs. 22, 36, and 37, ensures that RPMD reaction rates provide a good approximation to quantum thermal rates in the absence of substantial quantum coherence [38, 39]. RPMD rates can be computed using the Bennett–Chandler approach [40], which expresses the thermal rate as the product

$$k(T) = \kappa(t_p) k_{\text{QTST}}(T), \quad (4)$$

where $k_{\text{QTST}}(T)$ is the quantum transition-state theory rate [36, 41] and $\kappa(t_p)$ is the dynamical transmission coefficient. The latter is calculated as the value of the flux-side correlation function at a plateau time t_p [38, 39]. Equation (4) relies on a separation of timescales between the recrossing dynamics and the reaction [42]. For low-barrier systems, where this assumption may not hold, a modified expression can be used instead, given in Ref. [27] and in the Supplemental Material (SM) [43].

Friction.—To incorporate electronic friction into RPMD, we consider a potential energy function of the form

$$V(\mathbf{q}) = V^{\text{ext}}(Q) + \sum_{\nu=1}^{n_{\text{bath}}} \frac{m\omega_{\nu}^2}{2} \left[q_{\nu} - \frac{c_{\nu}F(Q)}{m\omega_{\nu}^2} \right]^2, \quad (5)$$

where $(P, Q) \equiv (p_0, q_0)$ denotes the nuclear coordinates—here taken to be one-dimensional—of a species with mass m . $V^{\text{ext}}(Q)$ denotes the Born–Oppenheimer potential energy surface, and the sum over ν represents the coupling to a bath of harmonic oscillators. The mapping of the dissipative environment onto a harmonic system-bath potential is general; it does not assume that the dissipative environment is itself harmonic [44]. The coupling coefficients c_{ν} and the bath frequencies ω_{ν} are encoded in the spectral density

$$J(\omega) = \frac{\pi}{2} \sum_{\nu=1}^{n_{\text{bath}}} \frac{c_{\nu}^2}{m\omega_{\nu}} \delta(\omega - \omega_{\nu}) \quad (6)$$

or, equivalently, the spectrum

$$\Lambda(\omega) = J(\omega)/\omega. \quad (7)$$

The friction kernel $\eta(Q, t, t')$ is proportional to the cosine transform of $\Lambda(\omega)$, as defined in the SM [43]. Any physical friction can be accurately represented using a sufficiently large n_{bath} . In this study, we obtain the spectrum $\Lambda(\omega)$ and the interaction potential $F(Q)$ from *ab initio* DFT calculations, identifying $F(Q)^2\Lambda(\omega)$ with Eq. (14) of Ref. [45], as implemented in the FHI-aims electronic structure package.

The system-bath Hamiltonian in Eq. (5) can be constructed by a direct harmonic discretization of the spectral density [46] and ring-polymerized as in Eq. (2). This approach provides an “explicit” representation of the dissipative environment in RPMD, which was employed by Bridge *et al.* in a previous study comparing dissipative RPMD rates to exact quantum benchmarks [24]. The explicit representation requires a large number of bath modes to converge the dissipative dynamics, introducing a prohibitive computational overhead.

Path-Integral GLE.—To reduce the computational overhead, we solve for the motion of the harmonic bath modes analytically, as done in Ref. 27 for position-independent friction, *i.e.*, $F(Q) = Q$. In the SM [43], we present all equations of motion for a general $F(Q)$, which encompasses position-dependent friction. We formulate the path-integral GLE in ring-polymer “normal-mode” coordinates, $\tilde{\mathbf{Q}} = (\tilde{Q}^{(0)}, \tilde{Q}^{(\pm 1)}, \tilde{Q}^{(\pm 2)}, \dots)$. These are the normal modes of a free ring-polymer (V_{sys} is constant), which are known analytically and used routinely in RPMD calculations. Their definition is given in the SM [43] along with the derivation of the ring-polymer GLE.

The dissipative bath renormalizes the ring-polymer potential, leading to

$$\tilde{V}_N^{\text{ren}}(\tilde{\mathbf{Q}}) = \tilde{V}_N^{\text{sys}}(\tilde{\mathbf{Q}}) + \frac{1}{2} \sum_n \alpha^{(n)} [\tilde{F}^{(n)}]^2, \quad (8a)$$

$$\alpha^{(n)} = \frac{2}{\pi} \int_0^\infty \frac{\Lambda(\omega) \tilde{\omega}_n^2}{\omega^2 + \tilde{\omega}_n^2} d\omega, \quad (8b)$$

where \tilde{V}_N^{sys} is the potential of an N -bead ring polymer in the absence of friction, $\tilde{F}^{(n)}$ are normal-mode interaction potentials, related to $\{F(Q^{(0)}), F(Q^{(1)}), \dots, F(Q^{(N-1)})\}$ by a linear transformation, and

$$\tilde{\omega}_n = \frac{2N}{\beta\hbar} \sin\left(\frac{\pi|n|}{N}\right) \quad (9)$$

are the harmonic frequencies associated with normal modes $\tilde{Q}^{(\pm n)}$. Equation (8) is a reformulation of Eq. (34) in Ref. [16]. It accounts for the suppression of tunnelling probability and is the only modification needed to obtain the QTST rate $[k_{\text{QTST}}(T)$ in Eq. (4)] in the presence of friction.

The dynamical transmission coefficient $[\kappa(t_p)$ in Eq. (4)] is further influenced by the dissipative and stochastic forces acting on the normal-mode momenta $\tilde{P}^{(n)}$. These forces are described by the GLE

$$\begin{aligned} \frac{d\tilde{P}^{(n)}}{dt} = & -\frac{\partial \tilde{V}_N^{\text{ren}}}{\partial \tilde{Q}^{(n)}} - \int \sum_{n'} \eta^{(n,n')}(t, t'; \tilde{\mathbf{Q}}) \frac{\tilde{P}^{(n')}(t')}{m} dt' \\ & + \sum_{n'} \frac{\partial \tilde{F}^{(n)}(t)}{\partial \tilde{Q}^{(n')}} \zeta^{(n')}(t), \end{aligned} \quad (10)$$

where the ring-polymer friction tensor is given by

$$\eta^{(n,n')}(t, t'; \tilde{\mathbf{Q}}) = \sum_{n''} \frac{\partial \tilde{F}^{(n'')}(t)}{\partial \tilde{Q}^{(n)}} K^{(n'')}(t-t') \frac{\partial \tilde{F}^{(n'')}(t')}{\partial \tilde{Q}^{(n')}}, \quad (11)$$

and the “resolvent” associated with $\tilde{P}^{(n)}$ is

$$K^{(n)}(t) = \frac{2}{\pi} \int_0^\infty \frac{\Lambda(\omega) \omega^2}{\omega^2 + \tilde{\omega}_n^2} \cos\left(t\sqrt{\omega^2 + \tilde{\omega}_n^2}\right) d\omega. \quad (12)$$

The stochastic forces $\zeta^{(n)}$ satisfy the second fluctuation-dissipation theorem [47]

$$\langle \zeta^{(n)}(t) \zeta^{(n)}(t') \rangle = k_B T K^{(n)}(t-t'). \quad (13)$$

For simplicity, all expressions are given for a one-dimensional system but can be straightforwardly generalized to the multidimensional case.

For the centroid coordinate $\tilde{P}^{(0)}$, the normal-mode frequency $\tilde{\omega}_0 = 0$, so that the centroid resolvent $K^{(0)}(t)$ is identical to the resolvent of the classical GLE. For a constant friction spectrum $[\Lambda(\omega) = \text{const.}]$ the centroid resolvent produces a Markovian friction, $K^{(0)}(t) \propto \delta(t)$. The

other resolvents have a more complicated time dependence, even for constant $\Lambda(\omega)$ [27], and will always generate non-Markovian friction. To propagate the dissipative dynamics, we map the non-Markovian GLE onto a system of multivariate Ornstein–Uhlenbeck equations [48]. The mapping consists in coupling n_{aux} pairs of fictitious auxiliary dynamical variables to every momentum coordinate. The coupling parameters are fitted so that the interactions with the auxiliary variables reproduce the dissipative and random forces in Eq. (10) (see SM [43] for details of the parametrization and propagation). This approach generalizes the path-integral stochastic thermostatting algorithm [28–30], and requires only a few auxiliary variables ($n_{\text{aux}} \ll n_{\text{bath}}$) to converge the dissipative dynamics, significantly reducing the computational overhead.

Reaction Model.—To study the diffusion of atomic hydrogen on Cu(111), we mapped the potential connecting the *hcp* and *fcc* adsorption sites [Fig. 1(a,b)]. We considered the effects of surface relaxation, basis set and choice of functional on the potential energy curve and corresponding rates, as reported in the SM [43]. In the following, we show results for a substrate lattice that was fixed at the bare-slab equilibrium geometry. For the mapping, the hydrogen atom was constrained at equidistant points along the line connecting the two adsorption sites, optimizing the displacement perpendicular to the slab surface. We calculated the potential energy using DFT with the PBE exchange-correlation functional [49] and the Tkatchenko–Scheffler screened van der Waals dispersion corrections [50], as implemented in FHI-aims [51] (see the SM [43]). The electronic friction was computed from the electron-phonon coupling matrix elements, also obtained using FHI-aims [45]. Deviations of the interaction potential $F(Q)$ from linearity were negligible for this system, and all results presented below were derived from simulations using the linear approximation, $F(Q) = Q$. Dynamical simulations were performed with an in-house code [52], where the algorithms developed in this letter were implemented for one-dimensional potential energy profiles.

QTST Rates.—In a typical calculation, the “raw” *ab initio* electronic friction spectrum is convolved with a Gaussian window of width σ to extrapolate to the infinitely large k -grid limit. In order to approximate the friction as Markovian, σ is set to be large, typically between 0.3 eV and 0.6 eV. However, this washes out the spectral detail at the low energy scales relevant to surface diffusion. A narrower window [Fig. 1(c) and (d)] reveals that for hydrogen on Cu(111) electronic friction is super-Ohmic [53] at low energies. This feature has a significant impact on calculated reaction rates. The choice of σ directly impacts the renormalized ring-polymer potential in Eq. (8), which modulates tunnelling probabilities and the computed QTST rates.

Using the renormalized ring-polymer potential instead of the system-bath representation in Eq. (5) greatly accelerated the convergence of QTST rate calculations. The acceleration is twofold: firstly, there are many fewer degrees of freedom to propagate, so that the computational cost of a single propagation step is reduced. Secondly, we are not explicitly sampling the thermal distribution

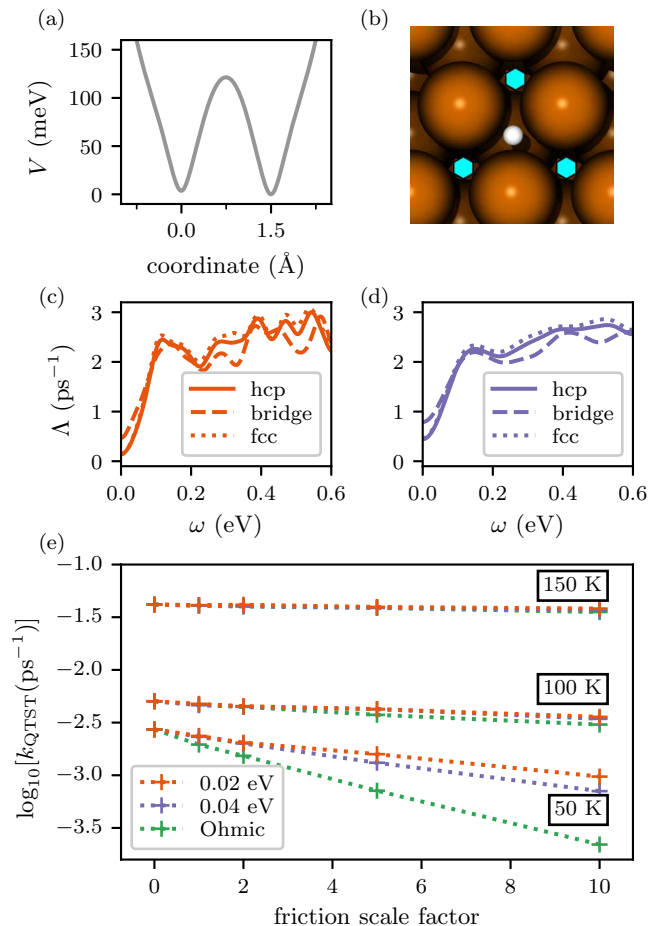


FIG. 1. (a) Potential energy along the reaction coordinate connecting the *hcp* site of Cu(111) at 0 \AA and the *fcc* site at 1.5 \AA , computed using DFT with the PBE exchange–correlation functional and Tkatchenko–Scheffler screened van der Waals correction (see SM [43]). (b) Hydrogen atom adsorbed at the *hcp* site of Cu(111), with the three neighbouring *fcc* sites marked by blue hexagons. (c) Spectra of the electronic-friction tensor projected onto the reaction coordinate and convolved with a $\sigma = 0.02 \text{ eV}$ Gaussian window. The solid, dashed, and dotted line show spectra at the reactant minimum (*hcp*), transition state (bridge) and product minimum (*fcc*), respectively. The *fcc* and *hcp* spectra are near identical. (d) Same, but for a $\sigma = 0.04 \text{ eV}$ window. (e) QTST rates for the potential in panel (a), coupled to a bath with either the *fcc* spectrum from panel (c), panel (d), or an Ohmic bath with $\eta_0 = 2 \text{ ps}^{-1}$. Rates are also shown for systems with rescaled friction, $\eta_{\text{scaled}}(Q, t, t') = \varsigma \eta(Q, t, t')$, where ς is the friction scale factor.

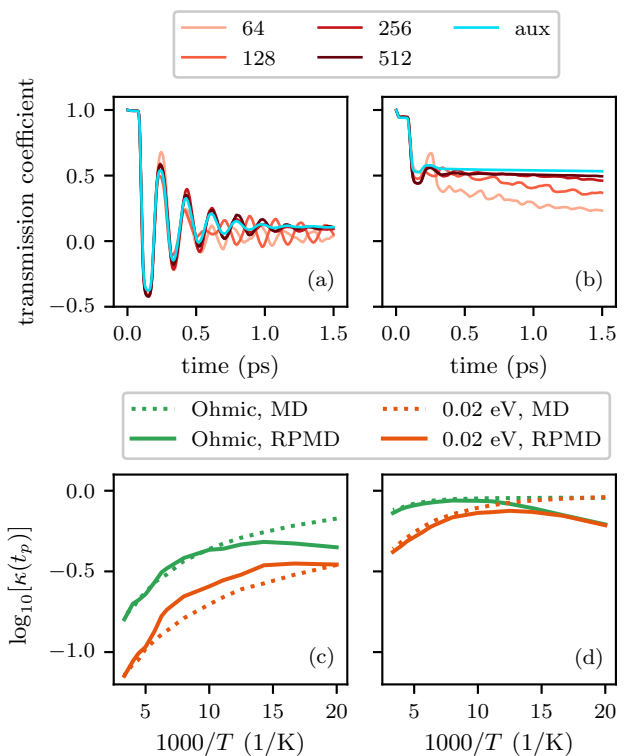


FIG. 2. (a) Classical ($N = 1$) transmission coefficient at 200 K for the *fcc* friction spectrum in Fig. 1(c) damped by $w(\omega) = e^{-\omega/\omega_c}$, $\omega_c = 4000 \text{ cm}^{-1}$. Calculations using harmonic bath discretization [46] are shown in shades of red (see legend for the number of bath modes). Simulation results using the auxiliary variable propagator with $n_{\text{aux}} = 5$ are shown in cyan. (b) Same but for friction scaled by a factor of 10. (c) Classical (MD) and ring-polymer (RPMD) transmission coefficients computed for the same friction spectrum as in panel (a) and an Ohmic friction with $\eta_0 = 2 \text{ ps}^{-1}$. (d) Same, but for friction scaled by a factor of 10.

of the harmonic bath modes, so that a given sampling accuracy is reached for a smaller total number of steps (see SM [43]). Simulation times in our study were reduced by a factor of 100 for some friction and temperature regimes.

To facilitate comparison with experimental results, all calculated QTST rates are multiplied by a factor of 3, in order to account for hops to all three equivalent neighbouring *fcc* sites [Fig. 1(b)]. For the *ab initio* friction, the relative differences between rates calculated with Ohmic and super-Ohmic profiles significantly increase when the friction strength is varied within the range spanned by typical metal substrates, as shown in Fig. 1(e). Thus, we predict that non-Markovian effects will have a stronger impact on low-temperature QTST rates for certain surfaces, e.g., Ru(0001) [32, 54],

Transmission coefficients.—The transmission coefficient $\kappa(t_p)$ is also strongly influenced by the low-frequency part of the friction spectrum. Calculating κ for our system is especially challenging due to the

weak damping exerted by the electronic friction, although we still expect RPMD to provide a good description of the quantum reaction rates, since quantum coherence should be negligible for low-frequency, low-barrier processes [24, 55]. However, weak friction results in a flux-side correlation function that is slow to reach a plateau. If one were to simulate the dissipative dynamics using a harmonic system-bath mapping in Eq. (5) and the discretization procedure in Ref. 46, over 500 modes would be needed to converge the calculation [Fig. 2(a) and (b)]. Simulations using the method of auxiliary variables to propagate the GLE in Eq. (10) reach convergence with only $n_{\text{aux}} = 5$.

As shown in Fig. 2(c) and (d), approximating electronic friction as Markovian leads to a substantial overestimation of the transmission coefficient. This can be attributed to the fact that, in the low-friction regime, the rate is limited by the efficiency of energy dissipation [18, 19]. The characteristic frequencies associated with the motion along the reaction coordinate are of $\mathcal{O}(50 \text{ meV})$, a spectral range where Ohmic friction exhibits enhanced spectral density compared to the actual friction spectra in Fig. 1(c). This results in Ohmic friction artificially enhancing energy dissipation, leading to an overestimation of the rate.

Overall rates.—A comparison of our low-friction calculation results with the *hcp*-site escape rates extracted from helium-3 surface spin-echo (HeSE) measurements by Townsend and co-workers [32] confirms that classical dynamics with Markovian friction provides a surprisingly good fit to the data, as noted previously [31]. However, a closer examination of the temperature dependence reveals the limitations of the classical model. Specifically, for hydrogen [Fig. 3(c)], the experimental rates at low temperatures ($< 200 \text{ K}$) exceed the predictions of a classical Arrhenius curve (see also Fig. S5 in the SM [43]). This discrepancy arises from the contribution of activationless deep tunnelling, which becomes the dominant reaction mechanism below the crossover temperature ($\approx 100 \text{ K}$). The onset of this effect is already apparent at the experimentally probed temperatures, indicating a non-classical behaviour that cannot be captured by the classical model alone.

In contrast to hydrogen, the experimental rates for deuterium [Fig. 3(d)] deviate from the linear Arrhenius trend in the opposite sense, falling slightly below the expected values at low temperatures. For this reaction, the crossover to deep tunnelling occurs around 70 K and does not significantly impact the temperature range in Fig. 3(d). However, the heavier mass of deuterium leads to RPMD rates converging on the classical predictions already at around 250 K , due to the diminishing importance of zero-point energy and shallow tunnelling effects [57, 58]. Consequently, the RPMD data for $T > 200 \text{ K}$, when fitted to a straight line, create the ap-

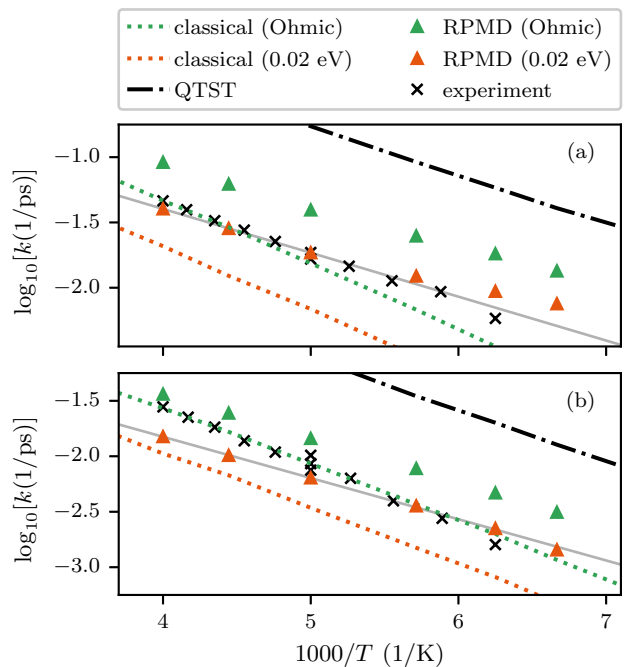


FIG. 3. (a) Hydrogen escape rates from the *hcp* site of Cu(111) for the potential in Fig. 1(a), computed using the same methods and friction profiles as in Fig. 2(c) and compared against HeSE measurements [32] (black crosses). The black dash-dotted line is the QTST rate, which is essentially identical with the semiclassical Wolynes rates [56] computed in Ref. 32. The grey line shows the linear Arrhenius fit to RPMD rates between 200 and 250 K. (b) Same as (a), but for deuterium on Cu(111).

pearance of a low-temperature rate “suppression”, mirroring the experimental observation.

Outlook.—In this letter, we described how non-Markovian friction effects can be incorporated into RPMD simulations using a GLE framework and an auxiliary-variable propagator algorithm. This method is readily applicable to multidimensional systems and it is generalizable to different types of frictional forces. It offers a practical tool for atomistic modelling, requiring only minor modifications to existing path-integral GLE infrastructure, such as that implemented in i-PI [59].

By applying this approach to the problem of hydrogen diffusion on Cu(111), we could study the interplay between friction memory and NQEs in reaction rates. Our results revealed that friction memory can significantly influence reaction rates above the tunnelling crossover temperature, effectively masking NQEs. This provides a nuanced understanding of the previously reported agreement between classical molecular dynamics and experiment [31], highlighting the importance of accurate electronic structure, NQEs, and dissipative dynamics for quantitative modelling. Furthermore, our auxiliary-variable GLE formulation is applicable to sys-

tems with strongly position-dependent friction, where we expect it to yield new physical insights [16, 17]. Combined with advances in embedding techniques [60, 61] and machine learning potentials [62], our method will be a powerful approach for studying reactions in metallic environments.

Acknowledgments.—We thank Yair Litman and Paolo Lazzaroni for our discussions of GLEs with position-dependent friction. We also thank Connor Box and Reinhard Maurer for their insightful advice on computing electronic friction. We are grateful to Paolo Lazzaroni for providing explicit system-bath benchmark RPMD rates. G.T. gratefully acknowledges a Research Fellowship from the Alexander von Humboldt Foundation.

* george.trenins@mpsd.mpg.de

- [1] V. Klippenstein, M. Tripathy, G. Jung, F. Schmid, and N. F. A. van der Vegt, Introducing Memory in Coarse-Grained Molecular Simulations, *J. Phys. Chem. B* **125**, 4931 (2021).
- [2] D. Antoniou and S. D. Schwartz, Quantum proton transfer with spatially dependent friction: Phenol-amine in methyl chloride, *J. Chem. Phys.* **110**, 7359 (1999).
- [3] M. Tuckerman and B. J. Berne, Vibrational relaxation in simple fluids: Comparison of theory and simulation, *J. Chem. Phys.* **98**, 7301 (1993).
- [4] K. Polley, K. R. Wilson, and D. T. Limmer, On the Statistical Mechanics of Mass Accommodation at Liquid-Vapor Interfaces, *J. Phys. Chem. B* **128**, 4148 (2024).
- [5] M. Head-Gordon and J. C. Tully, Molecular dynamics with electronic frictions, *J. Chem. Phys.* **103**, 10137 (1995).
- [6] M. Askerka, R. J. Maurer, V. S. Batista, and J. C. Tully, Role of Tensorial Electronic Friction in Energy Transfer at Metal Surfaces, *Phys. Rev. Lett.* **116**, 217601 (2016).
- [7] W. Dou and J. E. Subotnik, Perspective: How to understand electronic friction, *J. Chem. Phys.* **148**, 230901 (2018).
- [8] R. J. Maurer, M. Askerka, V. S. Batista, and J. C. Tully, Ab initio tensorial electronic friction for molecules on metal surfaces: Nonadiabatic vibrational relaxation, *Phys. Rev. B* **94**, 115432 (2016).
- [9] P. Spiering, K. Shakouri, J. Behler, G.-J. Kroes, and J. Meyer, Orbital-Dependent Electronic Friction Significantly Affects the Description of Reactive Scattering of N₂ from Ru(0001), *J. Phys. Chem. Lett.* **10**, 2957 (2019).
- [10] P. Spiering and J. Meyer, Testing Electronic Friction Models: Vibrational De-excitation in Scattering of H₂ and D₂ from Cu(111), *J. Phys. Chem. Lett.* **9**, 1803 (2018).
- [11] J. Gardner, S. Habershon, and R. J. Maurer, Assessing Mixed Quantum-Classical Molecular Dynamics Methods for Nonadiabatic Dynamics of Molecules on Metal Surfaces, *J. Phys. Chem. C* **127**, 15257 (2023).
- [12] R. P. Feynman, A. R. Hibbs, and D. F. Styer, *Quantum Mechanics and Path Integrals* (Dover Publications, 2010).
- [13] J. O. Richardson, Ring-polymer instanton theory, *Int. Rev. Phys. Chem.* **37**, 171 (2018).
- [14] Y. V. Suleimanov, F. J. Aoiz, and H. Guo, Chemical Reaction Rate Coefficients from Ring Polymer Molecular Dynamics: Theory and Practical Applications, *J. Phys. Chem. A* **120**, 8488 (2016).
- [15] D. Chandler and P. G. Wolynes, Exploiting the isomorphism between quantum theory and classical statistical mechanics of polyatomic fluids, *J. Chem. Phys.* **74**, 4078 (1981).
- [16] Y. Litman, E. S. Pócs, C. L. Box, R. Martinazzo, R. J. Maurer, and M. Rossi, Dissipative tunneling rates through the incorporation of first-principles electronic friction in instanton rate theory. I. Theory, *J. Chem. Phys.* **156**, 194106 (2022).
- [17] Y. Litman, E. S. Pócs, C. L. Box, R. Martinazzo, R. J. Maurer, and M. Rossi, Dissipative tunneling rates through the incorporation of first-principles electronic friction in instanton rate theory. II. Benchmarks and applications, *J. Chem. Phys.* **156**, 194107 (2022).
- [18] E. Pollak, H. Grabert, and P. Hanggi, Theory of activated rate processes for arbitrary frequency dependent friction: Solution of the turnover problem, *J. Chem. Phys.* **91**, 4073 (1989).
- [19] A. Nitzan, *Chemical Dynamics in Condensed Phases: Relaxation, Transfer and Reactions in Condensed Molecular Systems* (OUP Oxford, 2006).
- [20] E. Pollak, Instanton-based Kramers turnover theory, *Phys. Rev. A* **109**, 022242 (2024).
- [21] J. E. Lawrence, Semiclassical instanton theory for reaction rates at any temperature: How a rigorous real-time derivation solves the crossover temperature problem, *J. Chem. Phys.* **161**, 184115 (2024).
- [22] J. O. Richardson and S. C. Althorpe, Ring-polymer molecular dynamics rate-theory in the deep-tunneling regime: Connection with semiclassical instanton theory, *J. Chem. Phys.* **131**, 214106 (2009).
- [23] M. R. Fiechter, J. E. Runeson, J. E. Lawrence, and J. O. Richardson, How Quantum is the Resonance Behavior in Vibrational Polariton Chemistry?, *J. Phys. Chem. Lett.* **14**, 8261 (2023).
- [24] O. Bridge, P. Lazzaroni, R. Martinazzo, M. Rossi, S. C. Althorpe, and Y. Litman, Quantum rates in dissipative systems with spatially varying friction, *J. Chem. Phys.* **161**, 024110 (2024).
- [25] R.-H. Bi and W. Dou, Electronic friction near metal surface: Incorporating nuclear quantum effect with ring polymer molecular dynamics, *J. Chem. Phys.* **160**, 074110 (2024).
- [26] M. Ceriotti, M. Parrinello, T. E. Markland, and D. E. Manolopoulos, Efficient stochastic thermostating of path integral molecular dynamics, *J. Chem. Phys.* **133**, 124104 (2010), arXiv:1009.1045.
- [27] J. E. Lawrence, T. Fletcher, L. P. Lindoy, and D. E. Manolopoulos, On the calculation of quantum mechanical electron transfer rates, *J. Chem. Phys.* **151**, 114119 (2019), arXiv:1909.09882.
- [28] M. Ceriotti, G. Bussi, and M. Parrinello, Nuclear Quantum Effects in Solids Using a Colored-Noise Thermostat, *Phys. Rev. Lett.* **103**, 030603 (2009).
- [29] M. Ceriotti, G. Bussi, and M. Parrinello, Colored-Noise Thermostats à la Carte, *J. Chem. Theory Comput.* **6**, 1170 (2010).
- [30] M. Ceriotti and D. E. Manolopoulos, Efficient

- First-Principles Calculation of the Quantum Kinetic Energy and Momentum Distribution of Nuclei, *Phys. Rev. Lett.* **109**, 100604 (2012).
- [31] K. Gu, C. Li, B. Jiang, S. Lin, and H. Guo, Short- and Long-Time Dynamics of Hydrogen Spillover from a Single Atom Platinum Active Site to the Cu(111) Host Surface, *J. Phys. Chem. C* **126**, 17093 (2022).
- [32] P. S. M. Townsend, *Diffusion of Light Adsorbates on Transition Metal Surfaces*, Ph.D. thesis, University of Cambridge (2017).
- [33] G. X. Cao, E. Nabighian, and X. D. Zhu, Diffusion of Hydrogen on Ni(111) over a Wide Range of Temperature: Exploring Quantum Diffusion on Metals, *Phys. Rev. Lett.* **79**, 3696 (1997).
- [34] T. Firmino, R. Marquardt, F. Gatti, and W. Dong, Diffusion Rates for Hydrogen on Pd(111) from Molecular Quantum Dynamics Calculations, *J. Phys. Chem. Lett.* **5**, 4270 (2014).
- [35] I. R. Craig and D. E. Manolopoulos, Quantum statistics and classical mechanics: Real time correlation functions from ring polymer molecular dynamics, *J. Chem. Phys.* **121**, 3368 (2004).
- [36] T. J. H. Hele and S. C. Althorpe, Derivation of a true ($t \rightarrow 0^+$) quantum transition-state theory. I. Uniqueness and equivalence to ring-polymer molecular dynamics transition-state-theory, *J. Chem. Phys.* **138**, 084108 (2013), arXiv:1307.3729v1.
- [37] T. J. H. Hele, M. J. Willatt, A. Muolo, and S. C. Althorpe, Communication: Relation of centroid molecular dynamics and ring-polymer molecular dynamics to exact quantum dynamics, *J. Chem. Phys.* **142**, 191101 (2015), arXiv:1505.05065.
- [38] I. R. Craig and D. E. Manolopoulos, Chemical reaction rates from ring polymer molecular dynamics, *J. Chem. Phys.* **122**, 084106 (2005).
- [39] I. R. Craig and D. E. Manolopoulos, A refined ring polymer molecular dynamics theory of chemical reaction rates, *J. Chem. Phys.* **123**, 034102 (2005).
- [40] R. Collepardo-Guevara, I. R. Craig, and D. E. Manolopoulos, Proton transfer in a polar solvent from ring polymer reaction rate theory, *J. Chem. Phys.* **128**, 144502 (2008).
- [41] S. C. Althorpe and T. J. H. Hele, Derivation of a true ($t \rightarrow 0^+$) quantum transition-state theory. II. Recovery of the exact quantum rate in the absence of recrossing, *J. Chem. Phys.* **139**, 0 (2013), arXiv:1307.3020v2.
- [42] I. R. Craig, M. Thoss, and H. Wang, Proton transfer reactions in model condensed-phase environments: Accurate quantum dynamics using the multilayer multiconfiguration time-dependent Hartree approach, *J. Chem. Phys.* **127**, 144503 (2007).
- [43] See Supplemental Material at [URL will be inserted by publisher] for details of the DFT calculations; variations in the potential energy surface and rates upon surface relaxation and change of exchange-correlation functional; derivation of the ring-polymer GLE; details of the auxiliary variable propagation algorithm for the ring-polymer GLE; computational details and convergence test for the RPMD rate calculations. The Supplemental Material also includes Refs. [19, 26, 27, 42, 46–51, 53, 63–72].
- [44] A. Caldeira and A. Leggett, Quantum tunnelling in a dissipative system, *Ann. Phys.* **149**, 374 (1983).
- [45] C. L. Box, W. G. Stark, and R. J. Maurer, Ab initio calculation of electron-phonon linewidths and molecular dynamics with electronic friction at metal surfaces with numeric atom-centred orbitals, *Electron. Struct.* **5**, 035005 (2023).
- [46] P. L. Walters, T. C. Allen, and N. Makri, Direct determination of discrete harmonic bath parameters from molecular dynamics simulations, *J. Comput. Chem.* **38**, 110 (2017).
- [47] R. Kubo, The fluctuation-dissipation theorem, *Rep. Prog. Phys.* **29**, 306 (1966).
- [48] C. W. Gardiner, *Handbook of Stochastic Methods for Physics, Chemistry, and the Natural Sciences* (Springer-Verlag, 1985).
- [49] J. P. Perdew, K. Burke, and M. Ernzerhof, Generalized Gradient Approximation Made Simple, *Phys. Rev. Lett.* **77**, 3865 (1996).
- [50] V. G. Ruiz, W. Liu, E. Zojer, M. Scheffler, and A. Tkatchenko, Density-Functional Theory with Screened van der Waals Interactions for the Modeling of Hybrid Inorganic-Organic Systems, *Phys. Rev. Lett.* **108**, 146103 (2012).
- [51] V. Blum, R. Gehrke, F. Hanke, P. Havu, V. Havu, X. Ren, K. Reuter, and M. Scheffler, Ab initio molecular simulations with numeric atom-centered orbitals, *Comput. Phys. Commun.* **180**, 2175 (2009).
- [52] G. Trenins, <https://github.com/GeorgeTrenins/rpmd-gle/>.
- [53] U. Weiss, *Quantum Dissipative Systems (Fourth Edition)* (World Scientific, 2012).
- [54] N. Gerrits, J. I. Juaristi, and J. Meyer, Electronic friction coefficients from the atom-in-jellium model for $Z = 1 - 92$, *Phys. Rev. B* **102**, 155130 (2020).
- [55] M. R. Fiechter, J. E. Runeson, J. E. Lawrence, and J. O. Richardson, How Quantum is the Resonance Behavior in Vibrational Polariton Chemistry?, *J. Phys. Chem. Lett.* **14**, 8261 (2023).
- [56] P. G. Wolynes, Quantum Theory of Activated Events in Condensed Phases, *Phys. Rev. Lett.* **47**, 968 (1981).
- [57] R. Bell, *The Tunnel Effect in Chemistry* (Springer US, 2013).
- [58] J. O. Richardson, Microcanonical and thermal instanton rate theory for chemical reactions at all temperatures, *Faraday Discuss.* **195**, 49 (2016).
- [59] Y. Litman, V. Kapil, Y. M. Y. Feldman, D. Tisi, T. Begušić, K. Fidanyan, G. Fraux, J. Higer, M. Kellner, T. E. Li, E. S. Pócs, E. Stocco, G. Trenins, B. Hirshberg, M. Rossi, and M. Ceriotti, I-PI 3.0: A flexible and efficient framework for advanced atomistic simulations, *J. Chem. Phys.* **161**, 062504 (2024).
- [60] Q. Zhao, J. M. P. Martirez, and E. A. Carter, Revisiting Understanding of Electrochemical CO₂ Reduction on Cu(111): Competing Proton-Coupled Electron Transfer Reaction Mechanisms Revealed by Embedded Correlated Wavefunction Theory, *J. Am. Chem. Soc.* **143**, 6152 (2021).
- [61] X. Wen, J.-N. Boyn, J. M. P. Martirez, Q. Zhao, and E. A. Carter, Strategies to Obtain Reliable Energy Landscapes from Embedded Multireference Correlated Wavefunction Methods for Surface Reactions, *J. Chem. Theory Comput.* **20**, 6037 (2024).
- [62] H. J. Kulik, T. Hammerschmidt, J. Schmidt, S. Botti, M. A. L. Marques, M. Boley, M. Scheffler, M. Todorović, P. Rinke, C. Oses, A. Smolyanyuk, S. Curtarolo, A. Tkatchenko, A. P. Bartók, S. Manzhos, M. Ihara, T. Carrington, J. Behler, O. Isayev, M. Veit, A. Grisafi,

- J. Nigam, M. Ceriotti, K. T. Schütt, J. Westermayr, M. Gastegger, R. J. Maurer, B. Kalita, K. Burke, R. Nagai, R. Akashi, O. Sugino, J. Hermann, F. Noé, S. Pilati, C. Draxl, M. Kuban, S. Rigamonti, M. Scheidgen, M. Esters, D. Hicks, C. Toher, P. V. Balachandran, I. Tamblin, S. Whitelam, C. Bellinger, and L. M. Ghiringhelli, Roadmap on Machine learning in electronic structure, *Electron. Struct.* **4**, 023004 (2022).
- [63] L. Stella, C. D. Lorenz, and L. Kantorovich, Generalized Langevin equation: An efficient approach to nonequilibrium molecular dynamics of open systems, *Phys. Rev. B* **89**, 134303 (2014).
- [64] W. Liu, V. G. Ruiz, G.-X. Zhang, B. Santra, X. Ren, M. Scheffler, and A. Tkatchenko, Structure and energetics of benzene adsorbed on transition-metal surfaces: Density-functional theory with van der Waals interactions including collective substrate response, *New J. Phys.* **15**, 053046 (2013).
- [65] H. J. Monkhorst and J. D. Pack, Special points for Brillouin-zone integrations, *Phys. Rev. B* **13**, 5188 (1976).
- [66] J. Neugebauer and M. Scheffler, Adsorbate-substrate and adsorbate-adsorbate interactions of Na and K adlayers on Al(111), *Phys. Rev. B* **46**, 16067 (1992).
- [67] Y. Zhao and D. G. Truhlar, A new local density functional for main-group thermochemistry, transition metal bonding, thermochemical kinetics, and noncovalent interactions, *J. Chem. Phys.* **125**, 194101 (2006).
- [68] B. Oudot and K. Doblhoff-Dier, Reaction barriers at metal surfaces computed using the random phase approximation: Can we beat DFT in the generalized gradient approximation?, *J. Chem. Phys.* **161**, 054708 (2024).
- [69] M. Tuckerman, *Statistical Mechanics: Theory and Molecular Simulation* (OUP Oxford, 2010).
- [70] M. Ceriotti, *A Novel Framework for Enhanced Molecular Dynamics Based on the Generalized Langevin Equation*, Ph.D. thesis, ETH Zürich (2010).
- [71] I. S. Gradshteyn and I. M. Ryzhik, *Table of Integrals, Series, and Products*, edited by D. Zwillinger (Elsevier Science, 2014).
- [72] W. H. Press, S. A. Teukolsky, W. T. Vetterling, and B. P. Flannery, *Numerical Recipes: The Art of Scientific Computing*, 3rd ed. (Cambridge University Press, Cambridge, 2007).